

# A Novel Hybrid Beamforming Transmission Scheme for Common Channels and Signals

Xiaolin Hou, Huiling Jiang, Hidetoshi Kayama, Wei Xi  
 DOCOMO Beijing Communications Laboratories Co., Ltd.  
 Email: hou@docomolabs-beijing.com.cn

**Abstract**—Massive MIMO is envisioned as one of the key technologies for the 5th generation (5G) wireless communication systems. Hybrid beamforming is a promising and feasible solution to massive MIMO due to the achievable balance between performance and implementation cost, especially for the high frequency band. Different from user data channels and signals, common channels and signals cannot benefit from the user-specific beamforming gain, therefore, will suffer from a coverage issue due to the large propagation loss in the high frequency band. In order to provide an enhanced coverage for common channels and signals, in this paper we propose a novel hybrid beamforming transmission scheme, in which multiple analog beams are transmitted simultaneously via analog beamforming at the radio frequency (RF) front-end and cyclic shift (CS)-based beamforming is utilized in the digital back-end. With a proper CS setting, the received channel impulse responses (CIRs) from different beams can always be combined orthogonally. Therefore, a more stable and robust coverage of common channels and signals can be guaranteed. Both theoretical analysis and numerical evaluation justify its effectiveness.

**Index Terms**—hybrid beamforming; common channels and signals; coverage; cyclic shift

## I. INTRODUCTION

To satisfy the ever increasing demand of data throughput, both higher spectral efficiency and wider spectrum are desirable. Multi-input multi-output (MIMO) is a well-known solution to increase spectrum efficiency, i.e., improve the link capacity without the need of additional spectrum [1], and has been widely investigated. In recent years, even more antennas are considered at the transceivers for a more aggressive spectral efficiency enhancement, known as *massive MIMO* or *large scale MIMO* [2]–[4]. On the other hand, to meet the requirement of giga bits per second (Gbps) data transmission envisioned by the 5th generation (5G) of wireless communication systems, using wider spectrum, e.g. centimeter wave or millimeter wave, is also indispensable. Therefore, exploration of higher frequency bands (than the current cellular frequency band) has already been launched, including a variety of hardware experiments and measurement campaigns [5]–[7].

For data transmission in the high frequency band, one major challenge is how to conquer the larger propagation loss, less diffusion, and weaker penetration capability. Considering that higher frequency band has shorter wave length, given an array size, more antennas can be equipped to realize massive MIMO system and form narrower beams with larger beamforming gain to compensate the severe path loss. So the deployment of

massive MIMO over high frequency band provides an attractive solution for the 5G wireless communication systems [5].

Massive MIMO can realize beamforming in different ways, i.e., *digital beamforming* and *analog beamforming*. The former is performed in the digital baseband back-end [8]–[10], while the latter in the analog radio frequency (RF) front-end. Each approach has its own pros and cons. For digital beamforming, it can provide better beam steering precision, but it is more complex and expensive, since it requires separate baseband processing modules and power-hungry ADC/DAC converters for each antenna element (AE). On the other hand, analog beamforming is simpler and inexpensive, but less flexible. A reasonable compromise is to move some processing from digital baseband to analog RF at the cost of some flexibility loss in beam steering [11]. Thus, the concept of *hybrid beamforming* is proposed and quickly becomes one research focus in wireless communication [12].

A large number of research work has been done on hybrid beamforming [12]–[14], aiming to maximize the capacity or signal-to-noise power ratio (SNR) in single user case. While [15] focuses on the average transmit power minimization in multiuser transmission scenario. However, the majority of the research work only focus on the transmission of user data channels and signals, where user-specific beamforming can be designed to steer beams pointing to the expected user(s) and consequently the offered beamforming gain can compensate the severe propagation loss. But this is not the case for common channels and signals, e.g. system information, cell broadcast messages, discovery signals of small cells and phantom cells<sup>1</sup> [16], due to the fact that user-specific beamforming cannot be applied to common channels and signals. Therefore, how to guarantee an effective and robust coverage is critical for common channels and signals. To solve this problem, we propose a novel hybrid beamforming transmission scheme, in which multiple analog beams are transmitted simultaneously via analog beamforming at the radio frequency (RF) front-end and cyclic shift (CS)-based beamforming is utilized in the digital back-end. With a proper CS setting, the received channel impulse responses (CIRs) from different beams can always be combined orthogonally. Therefore, a more stable and robust coverage of common channels and signals can be guaranteed.

<sup>1</sup>For phantom cells, even though the majority of common channels and control signalings can be moved to their anchor macro cell, there are still some exceptions, e.g. discovery signals.

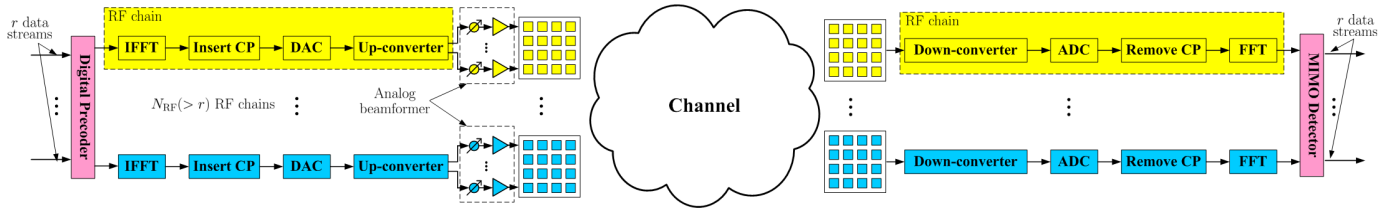


Fig. 1. An OFDM-based hybrid beamforming system

The remainder of this paper is structured as follows. In Section II, the background and system model are briefly introduced. In Section III, the proposed scheme is presented in details, and simulation results follow in Section IV. Finally, conclusions are drawn in Section V.

Throughout this paper, we adopt the following notational convention: Scalars are denoted by upper-case or lower-case plain letters, and their absolute values are expressed by  $\|\cdot\|$ . Vectors and matrices are expressed by lower-case boldface and upper-case boldface letters, respectively. Particularly,  $\mathbf{0}_L$  stands for a length- $L$  column vector, with all its elements equal 0.  $\text{diag}(\mathbf{v}_1 \ \mathbf{v}_2 \ \cdots \ \mathbf{v}_N)$  returns a block diagonal matrix with  $N$  vectors  $\mathbf{v}_1, \mathbf{v}_2, \dots, \mathbf{v}_N$  on its diagonal axis. Calligraphic upper-case letter  $\mathcal{C}$  with a subscript denotes a set, and  $|\cdot|$  returns its cardinality. For a random variable  $X$ ,  $\mathcal{P}_X(\cdot)$  is utilized to characterize its probability density function (PDF);  $\mathcal{E}(X)$  and  $\mathcal{V}(X)$  denote its expectation and variance, respectively.  $\mathcal{U}(a, b)$  stands for the uniform distribution between  $a$  and  $b$ ,  $a < b$ .  $\mathcal{CN}(0, \sigma^2)$  represents the zero mean circularly symmetric complex Gaussian (ZMCSG) distribution with variance  $\sigma^2$ .

## II. SYSTEM MODEL

Fig. 1 has illustrated the structure of an orthogonal frequency division multiplexing (OFDM)-based hybrid beamforming system. At the transmitter, as shown in the figure,  $r$  data streams are first precoded in digital baseband and then fed to the  $N_{\text{RF}}$  RF chains, including inverse fast Fourier transformation (IFFT), cyclic prefix (CP) insertion, digital-to-analog converter (DAC) and up-converter,  $r < N_{\text{RF}}$ . Each RF chain can drive a subarray, comprised of  $N_{\text{AE}}$  antenna elements, via a series of phase shifters and amplifiers.

Without loss of generality, we consider one stream of common channel or signal here, i.e.  $r = 1$ . For the sake of clear description, the digital and analog beamformers are denoted by  $\mathbf{d}(k)$  and  $\mathbf{A}$ , respectively, where  $k = 1, 2, \dots, N_{\text{FFT}}$  is the subcarrier index, and  $N_{\text{FFT}}$  is the FFT size or equivalently the number of subcarrier in OFDM system<sup>2</sup>. The digital beamformer  $\mathbf{d}(k)$  is a column vector of length  $N_{\text{RF}}$ , while the analog beamformer  $\mathbf{A}$  is a  $N_{\text{AE}}N_{\text{RF}} \times N_{\text{RF}}$  matrix. The overall beamforming vector for hybrid beamforming is the product of the both, i.e.  $\mathbf{A} \cdot \mathbf{d}(k)$ .

<sup>2</sup>In baseband back-end, digital beamforming can be flexibly controlled and consequently different from one subcarrier to another, while in one RF front-end, all the subcarriers have to share one analog beamforming vector.

For hybrid beamforming, considering the practical limitation of the beam steering at RF front-end, analog beamforming vectors are constrained within a predefined codebook  $\mathcal{C}_{\text{analog}}$ , comprised of a finite number of codewords. Moreover, in order to reduce the power consumption and cost, the number of RF chain is usually very limited and much smaller than the codebook size, i.e.,  $|\mathcal{C}_{\text{analog}}| > N_{\text{RF}}$ .

## III. TRANSMISSION SCHEMES FOR COMMON CHANNELS AND SIGNALS

In this section, conventional schemes are briefly introduced first for reference. Then, the proposed transmission scheme is presented in details.

### A. Conventional schemes

Concerning the transmission of common channels and signals, existing schemes can fall into three categories, termed as conventional scheme 1, 2 and 3, respectively.

For conventional scheme 1, only one RF chain is kept active while turning the others off. The corresponding analog beamformer can be written as

$$\mathbf{A}_{\text{conv1}} = \text{diag}(\mathbf{a} \ \underbrace{\mathbf{0}_{N_{\text{AE}}} \ \cdots \ \mathbf{0}_{N_{\text{AE}}}}_{N_{\text{RF}}-1}) \quad (1)$$

where  $\mathbf{a}$  is a length- $N_{\text{AE}}$  column vector standing for the analog beamforming weighting vector for one subarray driven by one RF chain. So for conventional scheme 1 (1), the directional coverage and beam width directly depend on the *array factor* of one subarray.

For conventional scheme 2, all the RF chains using one analog beamforming vector, i.e.,

$$\mathbf{A}_{\text{conv2}} = \text{diag}(\underbrace{\mathbf{a} \ \cdots \ \mathbf{a}}_{N_{\text{RF}}}) \quad (2)$$

Obviously, for conventional scheme 2 (2), only the coverage in the given beam direction can be improved due to the increased total transmit power.

In order to improve the coverage, a straightforward solution (conventional scheme 3) is to make each RF chain independently steer a beam, and different RF chains use different analog beamforming vectors. In this case, multiple beams can be transmitted simultaneously with analog beamformers as

$$\mathbf{A}_{\text{conv3}} = \text{diag}(\mathbf{a}_1 \ \mathbf{a}_2 \ \cdots \ \mathbf{a}_{N_{\text{RF}}}) \quad (3)$$

where  $\mathbf{a}_l$  is the analog beamforming vector for the subarray steered by  $l$ -th RF chain,  $\mathbf{a}_l \in \mathcal{C}_{\text{analog}}$ ,  $l = 1, 2, \dots, N_{\text{RF}}$ .

Compared to conventional schemes 1 and 2, conventional scheme 3 has better coverage performance. Its coverage is the combination of  $N_{\text{RF}}$  beams instead of one single beam. However, each beam may suffer the interference from its neighboring beams (as analyzed below). If a user lies in the coverage between two adjacent beams, the strength of the received signal will fluctuate remarkably, because the received beams from the both RF chains will combine either constructively or destructively. Moreover, the interference will become more severe as the number of RF chain  $N_{\text{RF}}$  increases.

In order to analyze the performance of conventional scheme 3, we consider a simple scenario where a user lies between two adjacent beams, corresponding to  $l$ -th and  $m$ -th RF chains, and the received signals from other  $(N_{\text{RF}} - 2)$  beams are very weak and can be neglected. The corresponding analog beamforming vectors of the two beams are  $\mathbf{a}_l$  and  $\mathbf{a}_m$ , respectively,  $\mathbf{a}_l, \mathbf{a}_m \in \mathcal{C}_{\text{analog}}$ . The total transmit power  $P_t$  is evenly distributed across the  $N_{\text{RF}}$  RF chains, i.e.  $P_t/N_{\text{RF}}$  for each chain. Without loss of generality, we assume that the channels from the both RF chains to the user are wide sense stationary uncorrelated scattering (WSSUS) channels. The corresponding channel impulse response (CIR) are denoted by independently and identically distributed (i.i.d.) ZMCSCG random variables, i.e.,

$$\begin{aligned} h_l(n) &\triangleq \|h_l(n)\|e^{j\alpha(n)} \sim \mathcal{CN}(0, \sigma_l^2(n)), \\ h_m(n) &\triangleq \|h_m(n)\|e^{j\beta(n)} \sim \mathcal{CN}(0, \sigma_m^2(n)), \end{aligned}$$

where  $\alpha(n)$  and  $\beta(n)$  are uniformly distributed phases in the range of  $[0, 2\pi)$ , i.e.  $\alpha(n), \beta(n) \sim \mathcal{U}(0, 2\pi)$ . The antenna gains of the both RF chains are denoted by  $G_l(n)$  and  $G_m(n)$ , respectively,  $n = 1, \dots, L$ , where  $L$  is the maximal delay spread.

In this case, the effective CIR can be written as

$$h_{\text{conv3}}^{\text{eff}}(n) = \sqrt{G_l(n)}h_l(n) + \sqrt{G_m(n)}h_m(n) \quad (4)$$

and the received power can be expressed by

$$\begin{aligned} P_{\text{conv3}} &= \frac{P_t}{N_{\text{RF}}} \sum_{n=1}^L \|h_{\text{conv3}}^{\text{eff}}(n)\|^2 \\ &= \frac{P_t}{N_{\text{RF}}} \sum_{n=1}^L G_l(n)\|h_l(n)\|^2 + G_m(n)\|h_m(n)\|^2 \\ &\quad + 2\sqrt{G_l(n)G_m(n)}\|h_l(n)\|\|h_m(n)\|\cos[\theta(n)] \end{aligned} \quad (5)$$

where  $\theta(n) \triangleq \alpha(n) - \beta(n) \sim \mathcal{U}(0, 2\pi)$ ,  $n = 1, 2, \dots, L$ . Since the effective CIR  $h_{\text{conv3}}^{\text{eff}}(n)$  in (4) is ZMCSCG distributed, i.e.  $h_{\text{conv3}}^{\text{eff}}(n) \sim \mathcal{CN}(0, G_l(n)\sigma_l^2(n) + G_m(n)\sigma_m^2(n))$ ,  $\|h_{\text{conv3}}^{\text{eff}}(n)\|^2$  is exponentially distributed with its PDF in (6). Therefore, the expectation and variance of  $P_{\text{conv3}}$  can be got as

$$\mathcal{E}(P_{\text{conv3}}) = \frac{P_t}{N_{\text{RF}}} \sum_{n=1}^L G_l(n)\sigma_l^2(n) + G_m(n)\sigma_m^2(n), \quad (7)$$

$$\mathcal{V}(P_{\text{conv3}}) = \frac{P_t^2}{N_{\text{RF}}^2} \sum_{n=1}^L [G_l(n)\sigma_l^2(n) + G_m(n)\sigma_m^2(n)]^2. \quad (8)$$

Obviously, as  $\theta(n)$  varies randomly,  $P_{\text{conv3}}$  fluctuates between an upper-bound and a lower-bound, which can be achieved when  $h_l(n)$  and  $h_m(n)$  combine constructively and destructively respectively, i.e., when  $\theta(n) = 0$  and  $\theta(n) = \pi$ ,  $n = 1, 2, \dots, L$ . The mean values of the upper-bound and lower-bound can be derived as

$$\begin{aligned} \mathcal{E}(P_{\text{conv3}}^{\text{ub}}) &= \frac{P_t}{N_{\text{RF}}} \sum_{n=1}^L G_l(n)\sigma_l^2(n) + G_m(n)\sigma_m^2(n) \\ &\quad + \frac{\pi}{2} \sqrt{G_l(n)G_m(n)}\sigma_l(n)\sigma_m(n) \end{aligned} \quad (9)$$

$$\begin{aligned} \mathcal{E}(P_{\text{conv3}}^{\text{lb}}) &= \frac{P_t}{N_{\text{RF}}} \sum_{n=1}^L G_l(n)\sigma_l^2(n) + G_m(n)\sigma_m^2(n) \\ &\quad - \frac{\pi}{2} \sqrt{G_l(n)G_m(n)}\sigma_l(n)\sigma_m(n) \end{aligned} \quad (10)$$

According to (9) and (10), it is clear that conventional scheme 3 does not perform as well as expected, because its coverage will vary randomly between the upper-bound and lower-bound. In other words, its coverage performance is neither stable nor robust.

### B. Proposed scheme

In order to avoid the destructive combination between adjacent beams, we introduce a joint design between both analog beamforming at the RF front-end and digital beamforming at the baseband back-end. This joint design contains two parts: On one hand, by analog beamforming, multiple analog beams are transmitted simultaneously; On the other hand, at digital beamforming stage, different RF chains can be configured with different CS values. The corresponding analog beamformer  $\mathbf{A}_{\text{prop}}$  is the same as in (3), but now additional digital beamformer is introduced

$$\mathbf{d}_{\text{prop}}(k) = \begin{bmatrix} e^{-j\frac{2\pi}{N_{\text{FFT}}}n_1k} \\ e^{-j\frac{2\pi}{N_{\text{FFT}}}n_2k} \\ \vdots \\ e^{-j\frac{2\pi}{N_{\text{FFT}}}n_{N_{\text{RF}}}k} \end{bmatrix} \quad (11)$$

where  $n_i$  is the CS value for  $i$ -th RF chain,  $i = 1, 2, \dots, N_{\text{RF}}$ . The basic principle can be illustrated by Fig. 2.

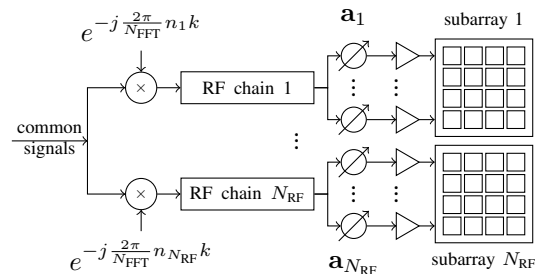


Fig. 2. Block diagram of the proposed hybrid beamforming scheme

For comparison, we consider the same scenario as in III.A. The only difference is that the both RF chains are configured with different CS values at digital beamforming stage, denoted

by  $n_l$  and  $n_m$ , respectively. Then, the effective CIR can be expressed by

$$h_{\text{prop}}^{\text{eff}}(n) = \sqrt{G_l(n)}h_l(n - n_l) + \sqrt{G_m(n)}h_m(n - n_m) \quad (12)$$

where  $h_l(n - n_l)$  and  $h_m(n - n_m)$  are  $n_l$ -sample and  $n_m$ -sample circularly shifted versions of  $h_l(n)$  and  $h_m(n)$ , respectively. The received signal power can be obtained by

$$\begin{aligned} P_{\text{prop}} &= \frac{P_t}{N_{\text{RF}}} \sum_{n=1}^L \|h_{\text{prop}}^{\text{eff}}(n)\|^2 \\ &= \frac{P_t}{N_{\text{RF}}} \sum_{n=1}^L \|\sqrt{G_l(n)}h_l(n - n_l) + \sqrt{G_m(n)}h_m(n - n_m)\|^2 \end{aligned} \quad (13)$$

If  $n_l$  and  $n_m$  are well designed,  $h_l(n - n_l)$  and  $h_m(n - n_m)$  will be orthogonal, and there is no overlapping between them in time domain. To satisfy the aforementioned condition, at most  $N_{\text{cs}} = \lfloor N_{\text{FFT}}/L \rfloor$  non-overlapped candidate CS values are available, i.e.,

$$C_{\text{cs}} = \left\{ i \frac{N_{\text{FFT}}}{N_{\text{cs}}} \mid i = 0, \dots, N_{\text{cs}} - 1 \right\} \quad (14)$$

Of course, among the RF chains with well-separated analog beams, CS values can be reused. Thus,  $P_{\text{prop}}$  can be further written as

$$\begin{aligned} P_{\text{prop}} &= \frac{P_t}{N_{\text{RF}}} \sum_{n=1}^L G_l(n)\|h_l(n)\|^2 + G_m(n)\|h_m(n)\|^2 \\ &= P_{\text{conv3}} \left( \|\theta_1\| = \dots = \|\theta_L\| = \frac{\pi}{2} \right) \end{aligned} \quad (15)$$

Clearly, for the proposed scheme, the received signal power is completely independent of the random and uncontrollable  $\theta(n)$ ,  $n = 1, 2, \dots, L$ . In other words, CS makes  $\|\theta_1\| = \dots = \|\theta_L\| = \pi/2$  irrespective of  $\alpha(n)$  and  $\beta(n)$ ,  $n = 1, 2, \dots, L$ .

It can be proved that  $\|h_{\text{prop}}^{\text{eff}}(n)\|^2$  is double-exponentially distributed with its PDF in (16), and we can obtain the mean value and variance of the received signal power  $P_{\text{prop}}$  as

$$\mathcal{E}(P_{\text{prop}}) = \frac{P_t}{N_{\text{RF}}} \sum_{n=1}^L G_l(n)\sigma_l^2(n) + G_m(n)\sigma_m^2(n), \quad (17)$$

$$\mathcal{V}(P_{\text{prop}}) = \frac{P_t^2}{N_{\text{RF}}^2} \sum_{n=1}^L G_l^2(n)\sigma_l^4(n) + G_m^2(n)\sigma_m^4(n) \quad (18)$$

By comparing (17) and (18) with (7) and (8), it can be clearly observed that concerning the received signal power, the proposed scheme has the same expectation as conventional scheme 3, but variance becomes smaller, i.e.  $\mathcal{E}(P_{\text{prop}}) = \mathcal{E}(P_{\text{conv3}})$  and  $\mathcal{V}(P_{\text{prop}}) < \mathcal{V}(P_{\text{conv3}})$ .

In summary, compared to the conventional schemes, the proposed method provides more stable and robust coverage

performance, which is of the most importance for the coverage of common channels and signals. In conventional scheme 3, the combination of two CIRs,  $h_l(n)$  and  $h_m(n)$ , depends on  $\theta(n)$  and is consequently uncontrollable. While in our proposed scheme, due to the introduction of CS, the CIRs are always combined orthogonally. In other words, the uncertainty and randomness of  $\theta(n)$  can be completely eliminated. This is just the reason why regarding the received signal power, the proposed scheme has smaller variance than conventional scheme 3.

#### IV. SIMULATION RESULTS

In order to evaluate the performance of the proposed transmission scheme for common channels and signals, numerical simulation is conducted in this section.

In our evaluation, we consider such a scenario that a base station (BS) is equipped with a 20-AE uniform linear array (ULA). The array can be further divided into two subarrays, each including 10 AEs and independently driven by a RF chain. The spacing between two adjacent AEs is 0.5 wavelength. The total transmit power is 46 dBm, and carrier frequency  $f_c$  is 3.5 GHz<sup>3</sup> [17]. The antenna gain and connector loss is 17 dBi. In the computation of distance-dependent path loss, line-of-sight (LOS) transmission is assumed, i.e.

$$PL(d) = 22 \log_{10}(d) + 28 + 20 \log_{10}(f_c) \quad \text{dB},$$

where  $d$  is the propagation distance. Regarding the array, the antenna pattern is

$$A(\phi) = -\min \left[ 12 \left( \frac{\phi}{\phi_{3\text{dB}}} \right)^2, A_m \right] \quad \text{dB},$$

where  $\phi_{3\text{dB}} = 70^\circ$  is the 3 dB beamwidth and  $A_m = 25$  dB is the maximal attenuation. The codebook for analog beamforming can be expressed as

$$C_{\text{analog}} = \left\{ \mathbf{r}(\theta) \mid \theta = 0, \pm \frac{\pi}{9} \right\},$$

where  $\mathbf{r}(\theta)$  is the *array response* of the antenna array, and  $\theta$  is the candidate angle of departure (AoD) available.

As mentioned in III-A, conventional scheme 3 outperforms conventional schemes 1 and 2 in coverage performance, therefore we only evaluate the performance of conventional scheme 3 for reference, and compare it with that of the proposed scheme. Moreover, for the sake of fair comparison, in our evaluation, total transmission power of the both schemes are equal. The performance metric is *effective coverage*, which is defined as a area in which the mean value of the received signal power keeps above a threshold, e.g. -40 dBm herein.

<sup>3</sup>Even though the performance evaluation is conducted over 3.5 GHz, the proposed scheme can be directly and flexibly extended to higher frequency bands, e.g. centimeter wave or millimeter wave.

$$\mathcal{P}_{\|h_{\text{conv3}}^{\text{eff}}(n)\|^2}(x) = \frac{N_{\text{RF}}}{P_t [G_l(n)\sigma_l^2(n) + G_m(n)\sigma_m^2(n)]} \cdot \exp \left\{ -\frac{N_{\text{RF}}x}{P_t [G_l(n)\sigma_l^2(n) + G_m(n)\sigma_m^2(n)]} \right\}, \quad x \geq 0; n = 1, \dots, L. \quad (6)$$

$$\mathcal{P}_{\|h_{\text{prop}}^{\text{eff}}(n)\|^2}(x) = \frac{N_{\text{RF}}}{P_t [G_l(n)\sigma_l^2(n) - G_m(n)\sigma_m^2(n)]} \cdot \left\{ \exp \left[ -\frac{N_{\text{RF}}x}{P_t G_l(n)\sigma_l^2(n)} \right] - \exp \left[ -\frac{N_{\text{RF}}x}{P_t G_m(n)\sigma_m^2(n)} \right] \right\}, \quad x \geq 0; n = 1, \dots, L \quad (16)$$

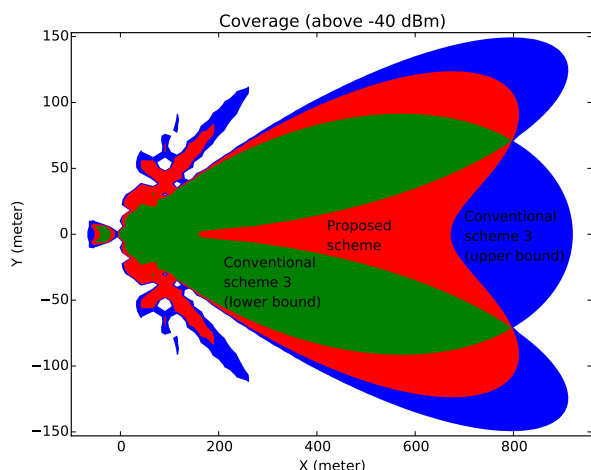


Fig. 3. The effective coverage of the proposed scheme and conventional scheme 3.

The effective coverage performance of the proposed scheme and conventional scheme 3 is illustrated in Fig. 3. According to the figure, the proposed scheme performs between the upper and lower bounds of conventional scheme 3 in (9) and (10), respectively. However, its coverage is much more stable and robust. Especially for the direction between the boresights of the both beams, the coverage performance is remarkably improved and enhanced, e.g. a stable coverage of about 700 meters far can be achieved.

## V. CONCLUSION

In this paper, an effective hybrid beamforming transmission scheme was proposed for common channels and signals, targeting at massive MIMO system deployed in high frequency band. By introducing the joint design between the RF front-end and the digital back-end, i.e. simultaneous transmission of multiple beams via analog beamforming together with CS-based digital beamforming in baseband, the coverage performance of common channels and signals can be enhanced, i.e., becomes more stable and robust. Both the theoretical analysis and numerical simulation justified its effectiveness. Further performance investigation with more realistic system-level simulation can be considered in our future work.

## REFERENCES

- [1] A. Paulraj, D. GORE, R. Nabar, and H. Bolcskei, "An overview of mimo communications - a key to gigabit wireless," *Proceedings of the IEEE*, vol. 92, no. 2, pp. 198–218, Feb 2004.
- [2] E. Larsson, O. Edfors, F. Tufvesson, and T. Marzetta, "Massive mimo for next generation wireless systems," *Communications Magazine, IEEE*, vol. 52, no. 2, pp. 186–195, February 2014.
- [3] L. Lu, G. Li, A. Swindlehurst, A. Ashikhmin, and R. Zhang, "An overview of massive mimo: Benefits and challenges," *Selected Topics in Signal Processing, IEEE Journal of*, vol. 8, no. 5, pp. 742–758, Oct 2014.
- [4] X. Gao, F. Tufvesson, and O. Edfors, "Massive mimo channels – measurements and models," in *Signals, Systems and Computers, 2013 Asilomar Conference on*, Nov 2013, pp. 280–284.
- [5] T. Rappaport, W. Roh, and K. Cheun, "Mobile's millimeter-wave makeover," *Spectrum, IEEE*, vol. 51, no. 9, pp. 34–58, Sept 2014.
- [6] W. Roh, J.-y. Seol, J. Park, B. Lee, J. Lee, Y. Kim, J. Cho, K. Cheun, and F. Aryanfar, "Millimeter-wave beamforming as an enabling technology for 5g cellular communications: theoretical feasibility and prototype results," *Communications Magazine, IEEE*, vol. 52, no. 2, pp. 106–113, 2014.
- [7] Z. Pi and F. Khan, "An introduction to millimeter-wave mobile broadband systems," *Communications Magazine, IEEE*, vol. 49, no. 6, pp. 101–107, June 2011.
- [8] S. Denno and T. Ohira, "Modified constant modulus algorithm for digital signal processing adaptive antennas with microwave analog beamforming," *Antennas and Propagation, IEEE Transactions on*, vol. 50, no. 6, pp. 850–857, Jun 2002.
- [9] F. Ellinger, U. Lott, and W. Bachtold, "Ultra low power gaas mmic low noise amplifier for smart antenna combining at 5.2 ghz," in *Radio Frequency Integrated Circuits (RFIC) Symposium, 2000. Digest of Papers. 2000 IEEE*, June 2000, pp. 157–159.
- [10] P. Karamalis, N. Skentos, and A. Kanatas, "Adaptive antenna subarray formation for mimo systems," *Wireless Communications, IEEE Transactions on*, vol. 5, no. 11, pp. 2977–2982, November 2006.
- [11] Y. Pei, T.-H. Pham, and Y.-C. Liang, "How many rf chains are optimal for large-scale mimo systems when circuit power is considered?" in *Global Communications Conference (GLOBECOM), 2012 IEEE*, Dec 2012, pp. 3868–3873.
- [12] J. Nsenga, A. Bourdoux, and F. Horlin, "Mixed analog/digital beamforming for 60 ghz mimo frequency selective channels," in *Communications (ICC), 2010 IEEE International Conference on*, May 2010, pp. 1–6.
- [13] J. Nsenga, W. Van Thillo, F. Horlin, V. Ramon, A. Bourdoux, and R. Lauwereins, "Joint transmit and receive analog beamforming in 60 ghz mimo multipath channels," in *Communications, 2009. ICC '09. IEEE International Conference on*, June 2009, pp. 1–5.
- [14] O. Ayach, R. Heath, S. Abu-Surra, S. Rajagopal, and Z. Pi, "Low complexity precoding for large millimeter wave mimo systems," in *Communications (ICC), 2012 IEEE International Conference on*, June 2012, pp. 3724–3729.
- [15] J. Geng, Z. Wei, X. Wang, W. Xiang, and D. Yang, "Multiuser hybrid analog/digital beamforming for relatively large-scale antenna arrays," in *Globecom Workshops (GC Wkshps), 2013 IEEE*, Dec 2013, pp. 123–128.
- [16] *DOCOMO 5G White Paper, 5G Radio Access: Requirements, Concept and Technologies*, July 2014.
- [17] 3GPP, *Evolved Universal Terrestrial Radio Access (E-UTRA); Further Advancements for E-UTRA Physical Layer Aspects*, ser. TR, no. TR36.814, Rel-9 v9.0.0. [Online]. Available: <http://www.3gpp.org/ftp/Specs/html-info/36814.htm>